**Article title:** The moisture distribution in wall-to-floor thermal bridges and its influence on mould growth

**Authors:** Yucong Xue[1], Yifan Fan[2], Jian Ge[3]
**Affiliations:** College of Civil Engineering and Architecture, Zhejiang University, China; Center of Balance Architecture, Zhejiang University, China; International Research Center for Green Building and Low-Carbon City, International Campus, Zhejiang University, Haining, China[1]
**Orcid ids:** 0000-0003-0891-3448[1]
**Contact e-mail:** yucongxue@zju.edu.cn



**Funder:** National Natural Science Foundation of China (NSFC); the Zhejiang Provincial Key R&D Program of China; the research project of the Ministry of Housing and Urban-Rural Development of China
**DOI:** 10.14324/111.444/000131.v1
**Preprint first posted online:** 06 March 2022
**Keywords:** Coupled heat and moisture transfer, Wall-to-floor thermal bridge, Moisture distribution, Mould growth, Built environment

# The moisture distribution in wall-to-floor thermal bridges and its influence on mould growth

Yucong Xue[1,2,3], Yifan Fan[1,2,3], Jian Ge[1,2,3*]

[1]College of Civil Engineering and Architecture, Zhejiang University, China

[2]Center of Balance Architecture, Zhejiang University, China

[3]International Research Center for Green Building and Low-Carbon City, International Campus, Zhejiang University, Haining, China

[*]Corresponding author: Jian Ge (gejian1@zju.edu.cn)

## Abstract

Moisture in the building envelopes increase the energy consumption of buildings and induce mould growth, which may be amplified within the area of thermal bridges due to their different hygrothermal properties and complex structures. In this study, we aimed to (1) reveal the moisture distribution in the typical thermal bridges (i.e., wall-to-floor thermal bridge, WFTB) and its surrounding area, and (2) investigate the mould growth in the building envelope that includes both WFTB and the main part of the wall. The transient numerical simulations that lasted for five years were performed to model the moisture distribution. Simulated results indicate that the moisture distribution presents significant seasonal and spatial differences due to the WFTB. The areas where moisture accumulates have a higher risk of mould growth. The thermal insulation layer laid on the exterior surface of WFTB can reduce the overall humidity while uneven moisture distribution, which may promote mould growth and water vapour condensation.

**Keywords:** Coupled heat and moisture transfer; Wall-to-floor thermal bridge; Moisture distribution; Mould growth

## 1. Introduction

The moisture content in envelopes impacts energy dissipation and water condensation by modifying both heat and moisture transfer characteristics in building envelopes. Such influence becomes more obvious when building envelopes are exposed to a hot-humid climate, such as the hot summer and cold winter climate zone in China [1]. The previous study has demonstrated that the cooling, heating and yearly load are significantly underestimated when the moisture transfer is neglected, revealing the importance of the analysis of coupled heat and moisture transfer [2]. Wang *et al.* investigated the thermal insulation performance of a typical thermal bridge (i.e., exterior corners) under steady-state conditions. The results indicate that the moisture transfer not only increases the heat dissipation of thermal bridges but also expands the influencing area [3]. Further, the phenomenon is significant with the increase in relative humidity [4].

The moisture in building envelopes not only affect the characteristics of heat transfer but also induces the mould growth and condensation of water vapour. Indoor mould growth is an important issue with critical implications, which may adverse health implications of heavy and systematic exposure to airborne fungal agents, especially in children [5]. The indoor organic pollutants caused by mould can also significantly decrease the service life of building materials and components [6]. Further, Mould growth is not limited to the indoor surface; it can easily germinate and expand inside building envelopes, mainly through condensation within a building form [7]. Unfortunately, the negative effects caused by moisture is more apparent in energy-efficient buildings due to some energy-saving methods, e.g., the application of thermal insulation layer [7]. However, the distribution of moisture within thermal bridges has not been paid enough attention, resulting in an incomprehensive understanding of the mould growth in these areas.

Based on the above research gaps, the objective of this study is to establish a model which is capable of simulating the coupled heat and moisture transfer (denoted as HAMT model) in a typical thermal bridge. The wall-to-floor thermal bridge (WFTB) occupies the largest area with the most massive heat flux [8, 9]. Therefore, the WFTB is employed as the object in our study to (1) reveal the moisture distribution, and (2) find high-risk areas for mould growth.

## 2. Theoretical models

As building materials are mostly composed of not only solid matrices but also pores, moisture will transfer in them together with heat. To describe the coupled process of heat and moisture transfer in building envelopes, the theoretical model is given in this section. On the basis of mass conservation law, the mass balance can be written as Eq. (1), which is finally converted to Eq. (2) with Fick's and Darcy's laws [10].

$$\frac{\partial \omega}{\partial t} = -\nabla\left(g_{\mathrm{l}} + g_{\mathrm{v}}\right) \tag{1}$$

$$\frac{\partial \omega}{\partial t} = \nabla\left(\left(\delta_{\mathrm{p}}\varphi\frac{dp_{\mathrm{sat}}}{dT}\right)\nabla T + \frac{\partial \varphi}{\partial p_{\mathrm{c}}}\left(D_{\mathrm{w}}\frac{\partial \omega}{\partial \varphi} + \delta_{\mathrm{p}}p_{\mathrm{sat}}\right)\nabla p_{\mathrm{c}}\right) \tag{2}$$

where $\omega$ is the gravimetric moisture content (kg·m$^{-3}$), $t$ the time coordinate (s), $g_{\mathrm{l}}$ the liquid flux (kg·m$^{-2}$·s$^{-1}$), $g_{\mathrm{v}}$ the vapour diffusion flux (kg·m$^{-2}$·s$^{-1}$), $\delta_{\mathrm{p}}$ the water vapour permeability (s), $\varphi$ the relative humidity, $p_{\mathrm{sat}}$ the saturated water vapour pressure (Pa), $T$ the temperature, $p_{\mathrm{c}}$ the capillary pressure (Pa), $D_{\mathrm{w}}$ the liquid water diffusivity (m$^2$·s$^{-1}$), $\rho_{\mathrm{l}}$ the density of liquid water (kg·m$^{-3}$), g the gravitational acceleration (m·s$^{-2}$).

According to energy conservation law, heat conduction and enthalpy flow caused by both vapour and liquid water transfer together constitute the energy change in the controlled element, as shown in Eq. (3). By combining with Fourier's law, the heat balance is then converted to Eq. (4).

$$\frac{\partial}{\partial t}\left(\rho c_{\mathrm{p}}T + h_{\mathrm{v}}\omega_{\mathrm{v}} + h_{\mathrm{l}}\omega_{\mathrm{l}}\right) = \nabla\left(-q - h_{\mathrm{v}}g_{\mathrm{v}} - h_{\mathrm{l}}g_{\mathrm{l}}\right) \tag{3}$$

$$\rho c_{\mathrm{p}}\frac{\partial T}{\partial t} = \nabla\left(\left(\lambda + h_{\mathrm{lat}}\delta_{\mathrm{p}}\varphi\frac{dp_{\mathrm{sat}}}{dT}\right)\nabla T + \left(h_{\mathrm{lat}}\delta_{\mathrm{p}}p_{\mathrm{sat}}\frac{\partial \varphi}{\partial p_{\mathrm{c}}}\right)\nabla p_{\mathrm{c}}\right) \tag{4}$$

where $\rho$ is the density of the building material under the absolutely dry condition (kg·m$^{-3}$), $c_{\mathrm{p}}$ the specific heat capacity of the material under the absolutely dry condition (J·kg$^{-1}$·K$^{-1}$), $\lambda$ the thermal conductivity (W·m$^{-1}$·K$^{-1}$), $h_{\mathrm{lat}}$ the latent heat of evaporation (J·kg$^{-1}$).

As the WFTB is a type of linear thermal bridge, two-dimension models are suitable for our study considering both accuracy and time efficiency. The two-dimensional formulation of Eqs. (2) and (4) can then be written as Eqs. (5) and (6).

$$\frac{\partial\omega}{\partial t}=\left(\delta_{\mathrm{p}}\varphi\frac{dp_{\mathrm{sat}}}{dT}\right)\left(\frac{\partial^2 T}{\partial x^2}+\frac{\partial^2 T}{\partial y^2}\right)+\frac{\partial\varphi}{\partial p_{\mathrm{c}}}\left(D_{\mathrm{w}}\frac{\partial\omega}{\partial\varphi}+\delta_{\mathrm{p}}p_{\mathrm{sat}}\right)\left(\frac{\partial^2 p_{\mathrm{c}}}{\partial x^2}+\frac{\partial^2 p_{\mathrm{c}}}{\partial y^2}\right) \tag{5}$$

$$\rho c_{\mathrm{p}}\frac{\partial T}{\partial t}=\left(\lambda+h_{\mathrm{lat}}\delta_{\mathrm{p}}\varphi\frac{dp_{\mathrm{sat}}}{dT}\right)\left(\frac{\partial^2 T}{\partial x^2}+\frac{\partial^2 T}{\partial y^2}\right)+\left(h_{\mathrm{lat}}\delta_{\mathrm{p}}p_{\mathrm{sat}}\frac{\partial\varphi}{\partial p_{\mathrm{c}}}\right)\left(\frac{\partial^2 p_{\mathrm{c}}}{\partial x^2}+\frac{\partial^2 p_{\mathrm{c}}}{\partial y^2}\right) \tag{6}$$

As the government equations are given above, the HAMT model is closed when the boundary conditions are introduced. Because both the wind-driven rain (WDR) and the convective vapour exchange can bring out the moisture flow, Eq. (7) are used to describe the process of moisture that flows from the environment to the surface of WFTB.

$$g=\beta\left(\varphi_{\mathrm{amb}}p_{\mathrm{sat,amb}}-\varphi_{\mathrm{sur}}p_{\mathrm{sat,sur}}\right)+\left(R_{\mathrm{WDR}}-R_{\mathrm{runoff}}\right) \tag{7}$$

where $g$ the total moisture flux (kg·m$^{-3}$), $\beta$ the vapour transfer coefficient at the surface (kg·Pa$^{-1}$·m$^{-2}$·s$^{-1}$), $\varphi_{\mathrm{amb}}$ and $\varphi_{\mathrm{sur}}$ the relative humidity of environment air and the surface, $p_{\mathrm{sat,amb}}$ and $p_{\mathrm{sat,sur}}$ the saturation water vapour pressure of environment air and the surface (Pa), $R_{\mathrm{WDR}}$ the moisture load caused by wind-driven rain (kg·m$^{-2}$·s$^{-1}$), $R_{\mathrm{runoff}}$ the excess water that runoff at the exterior surface (kg·m$^{-2}$·s$^{-1}$). It is assumed that there is no splash and runoff at the exterior surface of building envelopes, all the raindrops are absorbed and the $R_{\mathrm{runoff}}$ thus equals zero [11, 12]. Note that the last term on the right-hand side is zero when Eq. (7) is applied to the indoor side.

The heat flow across the surface comprises convective heat transfer, the latent heat transfer accompanied by the moisture flow, as well as the solar radiation, which is given as Eq. (8).

$$q=h\left(T_{\mathrm{amb}}-T_{\mathrm{sur}}\right)+h_{\mathrm{lat}}\beta\left(\varphi_{\mathrm{amb}}p_{\mathrm{sat,amb}}-\varphi_{\mathrm{sur}}p_{\mathrm{sat,sur}}\right)+\alpha I+\left(R_{\mathrm{WDR}}-R_{\mathrm{runoff}}\right)c_{\mathrm{p,l}}\left(T_{\mathrm{amb}}-T_{\mathrm{sur}}\right) \tag{8}$$

where $h$ is the convective heat transfer coefficient (W·m$^{-2}$·K$^{-1}$), $T_{\mathrm{amb}}$ and $T_{\mathrm{sur}}$ the temperature of environment air and the surface (K), $\alpha$ the solar absorptivity of the surface, $I$ the solar radiation (W·m$^{-2}$). It should be noted that the third and fourth terms on the right-hand side are equal to zero when Eq. (9) is applied to the indoor side.

### *2.2. Validation of the HAMT model*

The commercial software COMSOL Multiphysics [5.5.0.359, COMSOL, Inc., Stockholm, Sweden] is adopted to solve the above equations simultaneously. Before the HAMT model is applied, validation should be performed to ensure that the model has sufficient accuracy. The European Standard EN 15026: 2007 (Hygrothermal performance of building components and building elements) provides a normative benchmark with an analytical solution [13]. It is normally believed that the analytical solution is the exact solution for the PDEs, i.e., the analytical solution can accurately describe the transfer process of heat and moisture. Therefore, whether the HAMT model fulfils some basic requirements is identified in the following.

The moisture uptake in a thick single homogeneous material (semi-infinite region), which is assumed as perfectly airtight, is analysed in this benchmark. The initial condition of the material is 20 °C with a relative humidity of 50%, which is in equilibrium with the surrounding environment. At a certain time, the surrounding hygrothermal environment undergoes a step change (i.e., the temperature changes to 30 °C and the relative humidity changes to 95%). The material properties and other detailed descriptions are given in the European Standard EN 15026: 2007 [13]. The temperature and moisture profiles at different times are then be calculated, as shown in Fig. (1).

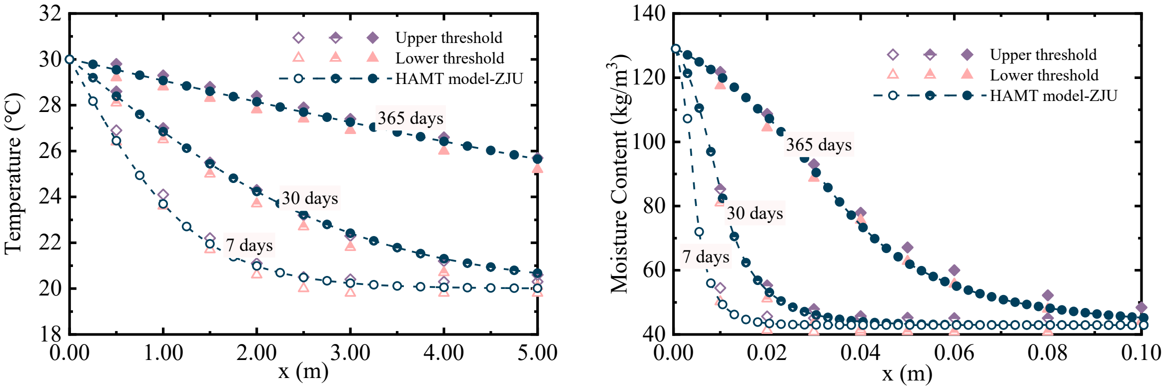


(a) (b)

**Fig. 1** Comparison between the numerical simulation results of the HAMT model and the analytical solution of EN 15026: 2007 in (a) temperature profile, and (b) moisture content profile at different times.

By comparing the numerical solution of the HAMT model with the upper/lower threshold produced by the analytical solution, it can be found that the good agreement in both temperature and moisture content is firmly proved, as Figs. 1(a) and (b) shows.

### *2.3. Case settings*

#### *2.3.1. Hygrothermal properties and configurations*

According to the existing atlas, Fig. 2 gives two configurations of the typical WFTB which is commonly used in residential buildings in the hot summer and cold winter climate zone of China [14]. The WFTB in Fig. 2(a) is insulated by an additional 20 mm layer of expanded polystyrene (EPS), while Fig. 2(b) is uninsulated. The cross-sections of WFTBs (see blue arrows in Fig. 5) are set as the adiabatic boundary condition, i.e., no energy and mass transfer here.

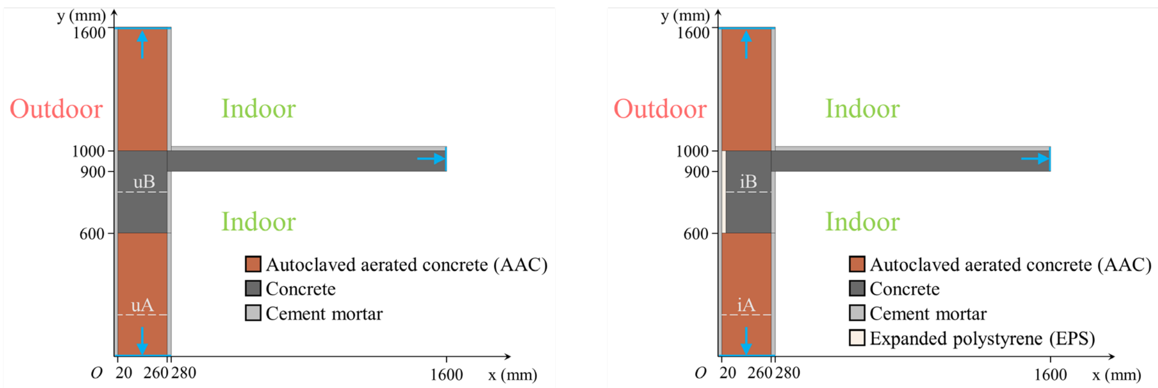


(a) (b)

**Fig. 2** Configurations of the WFTB: (a) uninsulated, and (b) insulated.

Following Kumaran [15], the hygrothermal properties of the building materials are listed in Table 1. Since the building materials are assumed as homogenous, all of the hygrothermal properties are uniform in both x- and y-directions. The solar absorptance of the surface $\alpha$ is set as 0.7 [16] and the initial condition for the WFTBs is $T$=293.15 K and $p_c$=135402728 Pa.

**Table 1** Hygrothermal properties of the building materials.

| Property | Concrete | AAC | Cement mortar | EPS |
|---|---|---|---|---|
| $\rho$ (kg·m$^{-3}$) | 2200 | 600 | 1512 | 25 |
| $c_p$ (J·kg$^{-1}$·K$^{-1}$) | 940 | 840 | 932 | 1470 |
| $\delta_p$ ($10^{-12}$ s) | 4.536 | 32.42 | 17.79 | 9.978 |
| $\lambda$ (W·m$^{-1}$·K$^{-1}$) | | $c_{\lambda 1} + c_{\lambda 2}\omega$ | | |
| $c_{\lambda 1}$ | 2.74 | 0.18 | 0.53 | 0.03 |
| $c_{\lambda 2}$ | 0.0032 | 0.00080 | 0.0031 | 0.0027 |
| $\omega$ (kg·m$^{-3}$) | | $c_{\omega 1}\varphi / \left[(1+c_{\omega 2}\varphi)\cdot(1-c_{\omega 3}\varphi)\right]$ | | |
| $c_{\omega 1}$ | 178.6 | 91670 | 219.3 | 9.566 |
| $c_{\omega 2}$ | 5.971 | 10690 | 8.731 | 9.237 |
| $c_{\omega 3}$ | 0.7598 | 0.9339 | 0.7414 | 0.3788 |
| $D_w$ (m$^2$·s$^{-1}$) | | $c_{Dw1}\cdot\exp(c_{Dw2}\omega_v)$ | | |
| $c_{Dw1}$ | $1.8\times10^{-11}$ | $9.2\times10^{-11}$ | $2.7\times10^{-9}$ | N/A |
| $c_{Dw2}$ | 0.0582 | 0.0215 | 0.0204 | |

"$c_{\lambda 1\text{-}2}$", "$c_{\omega 1\text{-}3}$", and "$c_{Dw1\text{-}2}$" are coefficients in the equations for thermal conductivity $\lambda$, moisture content $\omega$, and liquid diffusivity $D_w$, respectively.

### *2.3.2. Background conditions*

The indoor environment data and meteorological data last for a year in Hangzhou, a typical city in the HSCW climate zone, are adopted as the ambient conditions. For the indoor side, the ambient conditions (see Fig. 3-a) are collected from the record of an in-situ measurement in a residential building in Hangzhou (120.1 ºE, 30.3 ºN). For the outside, the meteorological data is recorded by a weather station (118.7 ºE, 29.5 ºN) and provided by commercial software WheatA [1.3.4, Xiaomaiya, Inc., Ningbo, China]. This group of data include temperature and relative humidity, global horizontal radiation, rainfall rate on a horizontal surface, and the speed and direction of the wind (see Fig. 3-b to -d). On the basis of the meteorological data, our seasons can then be divided by using the methods of meteorology and climatology: spring (from 1st Mar. to 31st May, i.e., 1417-3624 h), summer, known as the cooling season (from 1st June to 15th Sept., i.e., 3625-6192 h), autumn (from 16th Sept. to 15th Nov., i.e., 6193-7632 h), and winter, the heating season (from 16th Nov. to 28th May, i.e., 7633-8760 h and 1-1416 h) [17].

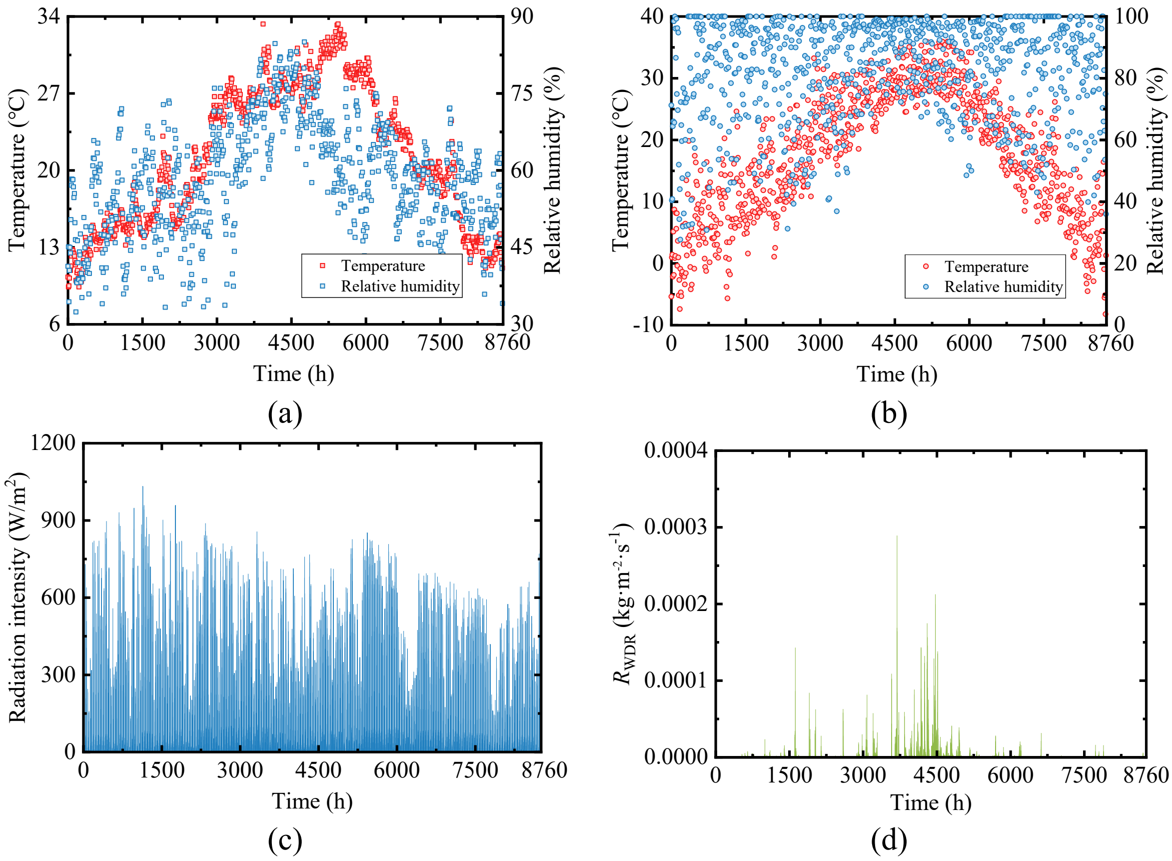


**Fig. 3** Ambient environment of WFTBs: (a) indoor temperature and relative humidity, (b) outdoor temperature and relative humidity, (c) radiation intensity $I$ at the eastward vertical wall, (d) moisture load caused by wind-driven rain $R_{\mathrm{WDR}}$ at the eastward vertical wall.

## *2.4. Evaluation indexes*

### *2.4.1. Average of relative humidity in building materials ($\varphi_{\mathrm{ave}}$)*

Since the environment parameters are obviously affected by seasons, the distribution of $\varphi$ in building envelopes has evident seasonal characteristics. Therefore, the average relative humidity in time domain $\varphi_{\mathrm{ave,t}}$, which can be calculated according to Eq. (9), is proposed to evaluate the overall relative humidity of building materials during a season. With the $\varphi_{\mathrm{ave,t}}$ for all areas of the WFTBs, a distribution of moisture can then be drawn, which is helpful to reveal the moisture accumulation area and provide guidance for mould and condensation proof.

$$\varphi_{\mathrm{ave,t}} = \frac{\int_k^j \varphi_i}{\int_k^j 1} \tag{9}$$

where $\varphi_i$ is the relative humidity at the time $i$, $j$ and $k$ are the range of the time domain that is used to calculate.

Based on the $\varphi_{\mathrm{ave,t}}$, the average of relative humidity in both time and space domains $\varphi_{\mathrm{ave,ts}}$ is further proposed to assess the overall moisture content in particular components, e.g., the thermal insulation layer, the WFTB. The $\varphi_{\mathrm{ave,ts}}$ is calculated according to Eq. (10).

$$\varphi_{\text{ave,ts}} = \frac{\int_k^j \int_n^m \varphi_{i,l}}{\int_k^j \int_n^m 1} \tag{10}$$

where $\varphi_{i,l}$ is the relative humidity at the time $i$ in position $l$, $m$ and $n$ are the range of the space domain that is used to calculate.

Thermal resistance $R$ ($m^2 \cdot K \cdot W^{-1}$) is widely used to evaluate the thermal performance of building envelope. After the $\varphi_{\text{ave,ts}}$ is calculated, the overall thermal resistance can then be figured out by using Eq. (11) and equations in Table 1.

$$R = \frac{\delta}{\lambda} \tag{11}$$

where $\delta$ *is* the thickness of the building envelope components (m).

### *2.4.2. Isopleth system for evaluation of mould risk*

In order to predict mould growth under transient boundary conditions, the Fraunhofer Institute of Building Physics (IBP) in Germany developed a bio-hygrothermal procedure, which is called the isopleth system [18]. Two groups of isolines are given by the system, one is used to predict the time required for spore germination (Fig. 4-1), and the other one is for the evaluation of mycelial growth (Fig. 4-1).

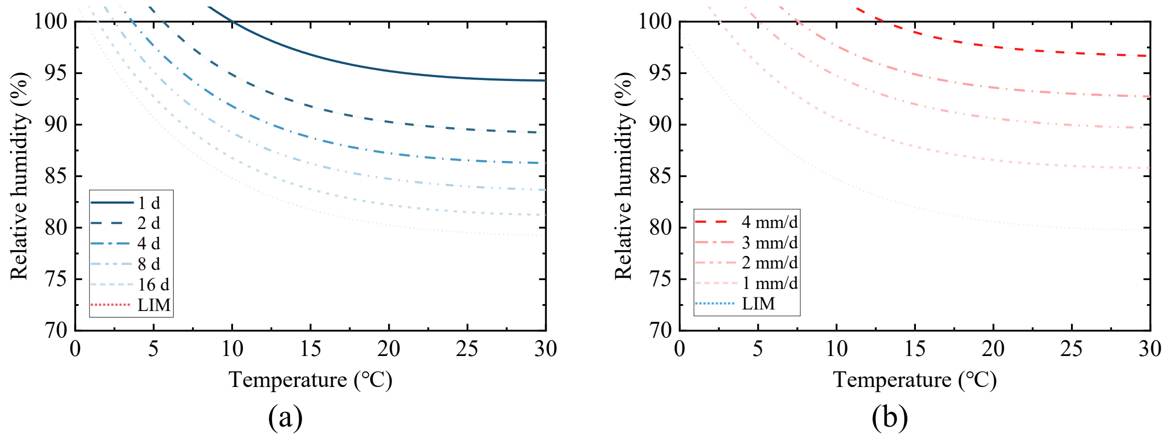


**Fig. 4** Isopleth systems for the biologically adverse recyclable building materials: (a) spore germination rate, and (b) mycelial growth rate.

For computational calculation purposes, each isoline needs to be converted into a mathematical form. Therefore, the two-term exponential is used to fit the isolines and the fitting results are listed in Table 3.

**Table 3** Coefficients for the equations in the isopleth system.

| $\varphi = ae^{bT_0} + ce^{dT_0}$ | | $a$ | $b$ | $c$ | $d$ |
|---|---|---|---|---|---|
| Spore germination | LIM | 24.37 | –0.1268 | 77.56 | 0.000486 |
| | $2^4$ d | 24.66 | –0.1265 | 79.39 | 0.000540 |
| | $2^3$ d | 23.94 | –0.1341 | 82.83 | 0.000163 |
| | $2^2$ d | 24.61 | –0.1237 | 84.14 | 0.000602 |
| | $2^1$ d | 25.01 | –0.1348 | 88.14 | 0.000247 |
| | $2^0$ d | 26.50 | –0.1205 | 91.35 | 0.000801 |

| | | | | | |
|---|---|---|---|---|---|
| Mycelial growth | LIM | 22.53 | –0.1120 | 76.59 | 0.001034 |
| | 1 mm/d | 22.26 | –0.1262 | 83.77 | 0.000601 |
| | 2 mm/d | 22.08 | –0.1295 | 88.43 | 0.000301 |
| | 3 mm/d | 23.99 | –0.1526 | 92.41 | 0.000030 |
| | 4 mm/d | 42.55 | –0.2052 | 97.44 | –0.000297 |

## 3. Results

For the purpose of eliminating the influence caused by the initial value, 5-year cyclic simulations for the process of heat and moisture transfer in this study has been performed. It should be noted that only the results in the fifth year (i.e., 35041-43800 h), which are still numbered as 1-8760 h, are used for analysis and the corresponding calculation.

### *3.1. Distribution of relative humidity*

The relative humidity contours at 1% intervals are drawn in Fig. 5, in which it can be found that when the components of building envelopes are not intersecting with the others (e.g., the main part of the wall), the contours are parallel to the surface, as the arrows in Fig. 5 show. When the properties of the component change or at the corner, the contours bend and may form a closed area. Such the closed area is called moisture sink when the $\varphi$ in the closed area is higher than the surrounding areas, while the opposite is called the moisture shadow. In Fig. 5, the areas of moisture sink ($A$) and the moisture shadow are 0.0531 and 0.0085 m$^2$, respectively. The difference between the maximum $\varphi$ in the moisture sink ($\varphi_{peak}$) and the $\varphi$ of the moisture sink boundary (denoted as $\boldsymbol{\varphi}_{\mathbf{max}}$) is 1.8%.

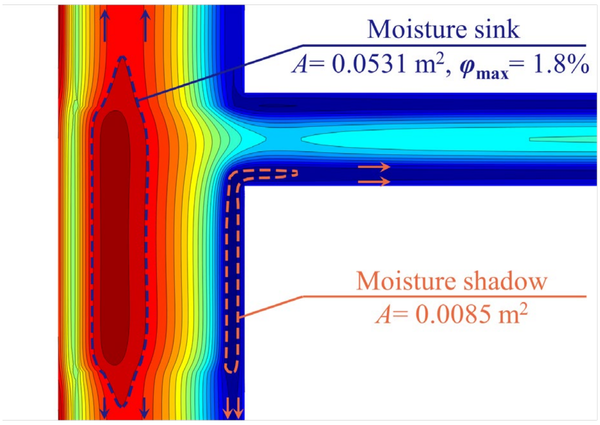


**Fig. 5** Illustration of the moisture sink and moisture shadow in WFTB (distribution of $\varphi$ at 6057 h).

Fig. 6(a) and (b) display the distribution of $\varphi_{ave,t}$ within WFTBs and their surrounding areas in the cooling and heating seasons, respectively. It should be noted that each figure is made up of the $\varphi_{ave,t}$ distributions in uninsulated and insulated WFTBs to easily compare the difference in different components.

Because the relative humidity of ambient air is higher during summer, the moisture content in WFTB is higher during the cooling season than that during the heating season. As a result, the $\varphi_{ave,ts}$s of the uninsulated WFTB are 72.5% and 67.0% in summer and winter, respectively; while the values of the insulated WFTB are 72.0% and 66.5%, respectively. It can be found that the $\varphi_{ave,ts}$ of the insulated WFTB is higher than that of the uninsulated one in general. In the study case, the relative humidity of outdoor air is generally higher than that of indoor air, i.e., the moisture transfers from outside to inside most of the time. Laying an insulation layer at the exterior surface of WFTB can isolate a part of inward moisture since the insulation material (expanded polystyrene. EPS) also has a function of moisture isolation. This process finally leads to relatively low humidity in the insulated WFTB.

In summer, by using Eqs. (10-11) and the hygrothermal properties provided by Table 1, the seasonal average of $R$ (denoted as $R_{ave,ts}$) of uninsulated and insulated WFTB are calculated as 0.0824 and 0.0755 $m^2 \cdot K \cdot W^{-1}$, respectively. When the season changes from summer to winter, the $R_{ave,ts}$s increases only by 0.0004 and 0.0005 $m^2 \cdot K \cdot W^{-1}$, respectively, which means that the change of seasons has a very limited effect on the thermal performance. However, the thermal conductivity ($\lambda$) of the concrete is 2.74 $W \cdot m^{-1} \cdot K^{-1}$ under the absolutely dry condition, i.e., the $R$s of the uninsulated and insulated WFTB is 0.0876 and 0.0803 $m^2 \cdot K \cdot W^{-1}$, respectively. Therefore, the $R_{ave,ts}$ of WFTB are reduced by 5.3% to 6.0%, which indicates the thermal insulation performance is obviously deteriorated due to the moisture.

The moisture sinks are reported in all four WFTBs in Fig. 6. Even though the overall relative humidity in the insulated WFTB is lower than that in the uninsulated one, the phenomenon of moisture sink is much more pronounced in the insulated WFTB, which can be reflected by a broader area (i.e., $A$) and a larger gradient (i.e., $\boldsymbol{\varphi}_{\mathbf{max}}$). Therefore, it can be said that the adoption of an insulation layer makes the moisture distribution more uneven, which may improve the risk of vapour condensation. Another noteworthy phenomenon is that the moisture shadows only appear at the interior surface of the WFTBs area during the cooling season, as Fig. 6(a) shows. This may reduce the risk of mould growth.

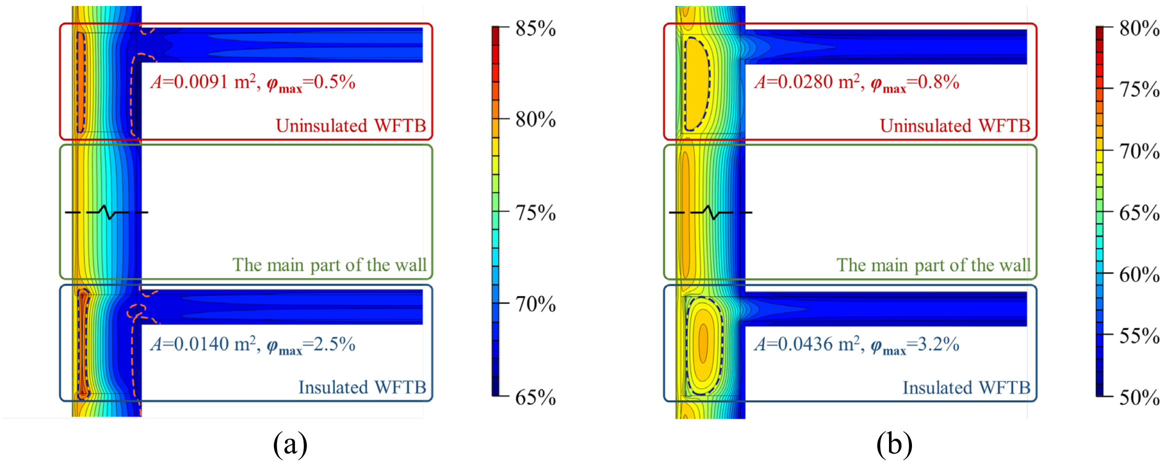


**Fig. 6** The distribution of $\varphi_{ave,t}$ within WFTBs and their surrounding areas in (a) summer, and (b) winter.

### *3.2. The mycelial growth in building envelopes*

When the temperature and relative humidity is appropriate (see Fig.4-a), mould spores will germinate at the surface or inside of the building envelopes [7]. After the spore germination, the mycelial will continue to grow if the hygrothermal environment is still within an acceptable range. It should be noted that the bacteriostatic effect of sunlight was not taken into consideration in this study.

Fig. 7 gives the rate of mycelial growth ($R_{MG}$) along different cross-sections. The uninsulated and insulated WFTBs are represented by cross-sections uB and iB, respectively. While both cross-section uA and cross-section iA represent the main part of the wall as this area has beyond the influence range of WFTBs. Consistent with common sense, because of the relatively high relative humidity of the environment with a suitable temperature, the most suitable period for mycelial growth is early summer, i.e., the plum rain season (from 29th May to 17th July, 3553-4751 h). Another period that mycelial grows rapidly is the time as summer moves to autumn, which is called "white dew" to "cold dew" (from 7th Sept. to 8th Oct., 5977-6744 h) in China's 24 solar terms. As the name implies, the water vapour in the air condenses easily due to the large temperature difference between day and night, which promotes spore germination and mycelial growth.

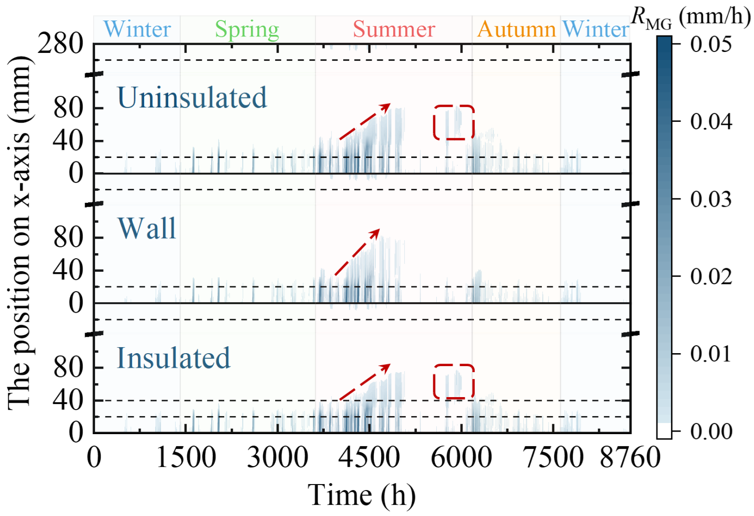


**Fig. 7** The growth rate of mycelial within different areas of building envelopes at all times of the year

Not only the season but also moisture distribution influence mycelial growth. As is said in Section 3.1., the moisture usually transfers from outside to inside, which results in the fact that the mould at the exterior surface grows earlier and faster than that inside the building envelopes (see the arrows in Fig. 7). However, due to the existence of moisture sinks (see Fig. 6-a), mycelial preferentially grows inside at some particular time, as the red boxes in Fig. 7 show. Moreover, the moisture shadows at the interior surfaces decrease the relative humidity and create conditions that are not conducive to mould growth. As a result, the $R_{MG}$ at the interior surface is higher within the wall area than that within the WFTB area, even though this phenomenon is not as apparent as the above one.

## 4. Discussion

The findings given by this study can enhance our understanding of how the moisture distributes in the building envelopes that include both WFTBs and the main part of the wall. It is obvious that laying a thermal insulation material outside the thermal bridge is beneficial to reduce the heat dissipation of the thermal bridges. This is not only because of the thermal isolating effect of such materials but also their function as a moisture barrier. The former can directly improve the thermal resistance of building envelopes, while the latter can prevent the thermal conductivity from increasing due to humidity by keeping the building envelopes dry. However, the application of exterior thermal insulation also causes some side effects that have not been revealed in previous studies. When the WFTB is externally insulated, the distribution of moisture content becomes more uneven, which may lead to higher risks of condensation of water vapour, spore germination, as well as mycelial growth. A hypothesis is put forward to explain this phenomenon: compared with the effect on moisture isolating, the insulation layer plays a greater role in thermal insulation. As a result, although both the moisture content and temperature in the insulated WFTB are lower than those in the uninsulated one, the influence of temperature plays a leading role, making the relative humidity higher. According to the above hypothesis, this phenomenon will become more obvious when the heat flow and moisture flow increase, which means the distribution of moisture is closely related to the orientation because of the different intensity of solar radiation and moisture load caused by wind-driven rain. Moreover, the effect of urban heat islands (UHI) during winter could also promote the occurrence of this phenomenon, i.e., the UHI not only influences the energy consumption of the heating, ventilation and air conditioning system in buildings but also has an inducing effect on vapour condensation and mould growth.

In future studies, a series of simulations with different thermal loads need to be performed to verify the above hypothesis. Meanwhile, practical methods should be further proposed to alleviate this phenomenon for the purpose of mould proof and condensation resistance. Moreover, the HAMT model can be further optimized for increasing the simulation accuracy, e.g., considering the influence caused by air leakage. The air flows through not only the inside of the porous materials but also the interface between different materials, with which the enthalpy flow also occurs inside the building envelopes and changes the energy and mass balance. Since the thermal bridges alter both the temperature and relative humidity on the building surfaces, their heat transfer characteristics affect not only the energy conservation of buildings but also building thermal plumes and the environment in street canyons, which is worthy of further investigation [19, 20].

## 5. Conclusion

In order to investigate the moisture distribution and predict the mould growth risk of the insulated and uninsulated wall-to-floor thermal bridges (WFTBs) as well as their surrounding areas, a coupled heat and moisture transfer model is developed and the process of heat and moisture transfer within the building envelopes is simulated. The average relative humidity in the time and space domain is proposed to evaluate the moisture distribution. While the isopleth system is adopted to predict the spore germination and mycelial growth. According to the results, the following conclusions are drawn:

(1) The moisture within the WFTBs deteriorates the thermal insulation performance by 5.3% to 6.0%, while the seasonal variation only has a very limited influence on the thermal performance.

(2) Due to the difference in hygrothermal properties of building envelope materials, there are areas where moisture accumulates (moisture sink) and areas where moisture disperse (moisture shadow).

(3) Laying a thermal insulation layer (expanded polystyrene, EPS) at the exterior surface of WFTB reduces the overall moisture content of WFTB. However, the moisture distribution becomes much more uneven when the EPS is used, which leads to apparent moisture sinks and moisture shadows.

(4) There are two most suitable periods of time for mould growth in a year, one is the plum rain season, and the other one is from “white dew” to “cold dew”.

(5) Under the influence of the moisture sink, mycelial preferentially grows inside at some particular time. While the moisture shadow can create conditions that are not conducive to mould growth

In accordance with the above conclusion, the thermal insulation for building envelopes should be reconsidered when the moisture transfer is taken into account. On one hand, the thermal insulation performance can no longer meet the requirements if the moisture transfer is considered. And on the other hand, the application of the thermal insulation layer also brings some side effects brought by, which have not been reported in the previous studies. Therefore, the combination of a thermal insulation layer and a vapour barrier membrane is recommended.

## Acknowledgement

This work was supported by the National Natural Science Foundation of China (NSFC) under Grant No. 52178093, the Zhejiang Provincial Key R&D Program of China under Grant No. 2021C03147. Yifan Fan acknowledge the research project of the Ministry of Housing and Urban-Rural Development of China (K20210466).

## Reference


[1] N. Mendes, F.C. Winkelmann, R. Lamberts, P.C. Philippi, Moisture effects on conduction loads, Energy Build. 35 (2003) 631-644, https://doi.org/10.1016/S0378-7788(02)00171-8.

[2] X. Liu, Y. Chen, H. Ge, P. Fazio, G. Chen, Numerical investigation for thermal performance of exterior walls of residential buildings with moisture transfer in hot summer and cold winter zone of China, Energy Build. 93 (2015) 259-268, https://dx.doi.org/10.1016/j.enbuild.2015.02.016.

[3] Y. Wang, Y. Fan, D. Wang, Y. Liu, J. Liu, The effect of moisture transfer on the inner surface thermal performance and the thermal transmittance of the roof-wall corner building node in high-temperature and high-humidity areas, J. Build. Eng. 44 (2021) 102949, https://doi.org/10.1016/j.jobe.2021.102949.

[4] Y. Wang, Y. Tian, Z. Zhao, D. Wang, Y. Liu, J. Liu, Effect of moisture transfer on heat transfer through exterior corners of cooled buildings in hot and humid areas, J. Build. Eng. 43 (2021) 103160, https://doi.org/10.1016/j.jobe.2021.103160.

[5] Y.D. Aktas, I. Ioannou, H. Altamirano, M. Reeslev, D. D'Ayala, N. May, M. Canales, Surface and passive/active air mould sampling: A testing exercise in a North London housing estate, Sci. Total. Environ. 643 (2018) 1631-1643, https://doi.org/10.1016/j.scitotenv.2018.06.311.

[6] Y.D. Aktas, J. Shi, N. Blades, D. D'Ayala, Indoor mould testing in a historic building: Blickling Hall, Herit. Sci. 6 (2018) 51, https://doi.org/10.1186/s40494-018-0218-x.

[7] A. Brambilla, A. Sangiorgio, Mould growth in energy efficient buildings: Causes, health implications and strategies to mitigate the risk, Renew. Sustain. Energy Rev. 132 (2020) 110093, https://doi.org/10.1016/j.rser.2020.110093.

[8] J. Ge, Y. Xue, Y. Fan, Methods for evaluating and improving thermal performance of wall-to-floor thermal bridges, Energy Build. 231 (2021) 110565, https://doi.org/10.1016/j.enbuild.2020.110565.

[9] J. Lu, Y. Xue, Z. Wang, Y. Fan, Optimised mitigation of heat loss by avoiding wall-to-floor thermal bridges in reinforced concrete buildings, J. Build. Eng. 30 (2020) 101214, https://doi.org/10.1016/j.jobe.2020.101214.

[10] H.M. Künzel, Simultaneous Heat and Moisture Transport in Building Components, Fraunhofer Institute of Building Physics, Holzkirchen, 1995, pp 14-15.

[11] A. Fang, Y. Chen, L. Wu, Modeling and numerical investigation for hygrothermal behavior of porous building envelope subjected to the wind driven rain, Energy Build. 231 (2021) 110572, https://doi.org/10.1016/j.enbuild.2020.110572.

[12] M. Abuku, H. Janssen, S. Roels, Impact of wind-driven rain on historic brick wall buildings in a moderately cold and humid climate: Numerical analyses of mould growth risk, indoor climate and energy consumption, Energy Build. 41 (2009) 101-110, https://doi.org/10.1016/j.enbuild.2008.07.011.

[13] British Standard Institution, Hygrothermal performance of building components and building elements_Assessment of moisture transfer by numerical simulation (BS EU 15026-2007), London, 2007.

[14] China Institute of Building Standard Design & Research, Structure of Autoclaved Aerated

Concrete (AAC) Blocks and Slabs (GJCT-016/06CG01), Beijing, 2007 (in Chinese).

[15] M.K. Kumaran, Heat, air and moisture transfer in insulated envelope parts: task 3 material properties, final report, International Energy Agency, Paris, 1996, pp. 25-84.

[16] J.P. Holman, Heat Transfer, China Machine Press, Beijing, 2015, pp. 379-485.

[17] Z. Yu, L. Wu, D. Gao, G. Fan, Investigation of methods for season division in Zhejiang Province, Meteorol. Sci. Technol. 42 (2014) 474-481, https://doi.org/10.19517/j.1671-6345.2014.03.019.

[18] E. Vereecken, S. Roels, Review of mould prediction models and their influence on mould risk evaluation, Build. Environ. 51 (2012) 296-310, https://doi.org/10.1016/j.buildenv.2011.11.003.

[19] Y. Fan, Y. Li, J. Huang, K. Wang, X. Yang, Natural convection flows along a 16-storey high-rise building, Build. Environ. 107 (2016) 215-225, https://doi.org/10.1016/j.buildenv.2016.08.003.

[20] Y. Fan, Y. Li, J. Hang, K. Wang, Diurnal variation of natural convective wall flows and the resulting air change rate in a homogeneous urban canopy layer, Energy Build. 153 (2017) 201-208, https://doi.org/10.1016/j.enbuild.2017.08.013.